SAND2019-3442PE

Interrogation of Plasma Discharges in Reacting Molecular and Supersonic Environments via Advanced Spectroscopic and Imaging Diagnostics

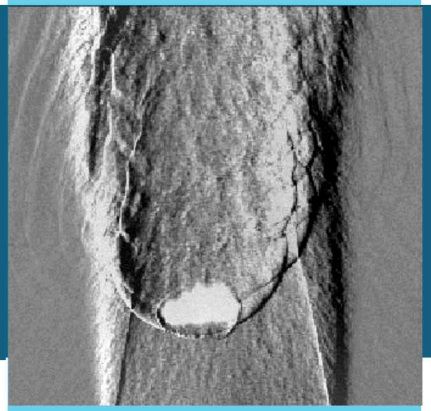

Caroline Winters, PhD

March 28th, Post-Doc Seminar

Sandia National Laboratories is a multimission laboratory managed and operated by National Technology & Engineering Solutions of Sandia, LLC, a wholly owned subsidiary of Honeywell International Inc., for the U.S. Department of Energy's National Nuclear Security Administration under contract DE-NA0003525.

SAND2019-0085 C

Nanosecond plasmas for flow actuation

- AC Surface-dielectric barrier discharge (AC-SDBD)
  - Diffuse and uniform plasmas
  - "Ionic wind" generates a body-force coupled with momentum in the external flow; (Corke et al., 2010)
- Arc filaments
  - High temperature, constricted plasmas
  - Flow control via heating → density change in the plasma affects mass balance of the system; (Leonov, 2004 & Webb et al., 2013)
  - Rapid localized heating generates strong compression wave; (Samimy et al., 2007 & Adamovich, 2009)
- Nanosecond pulsed plasma actuators:
  - Must be located at walls or jet exits
  - High repetition rates: $\tau \leq 100$ kHz
  - Strong scaling implications for large volume flows

AC-SDBD interacting with smoke

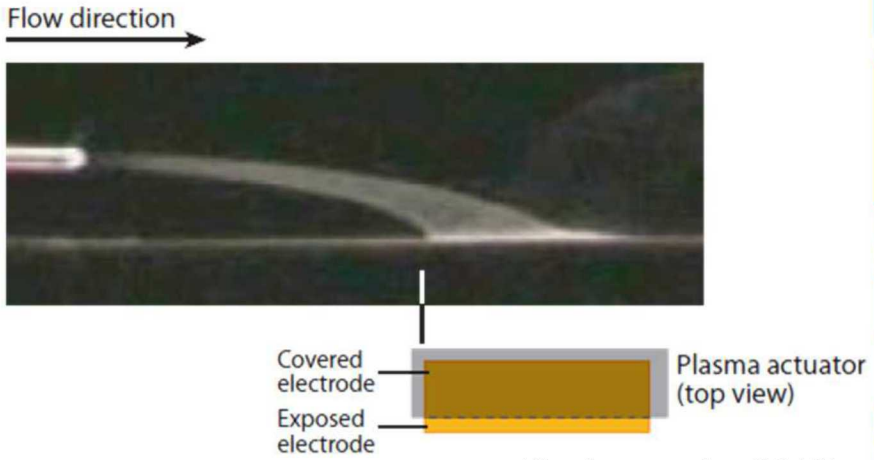

(Corke et al., 2010)

Four DC arc filament discharges interacting with a jet

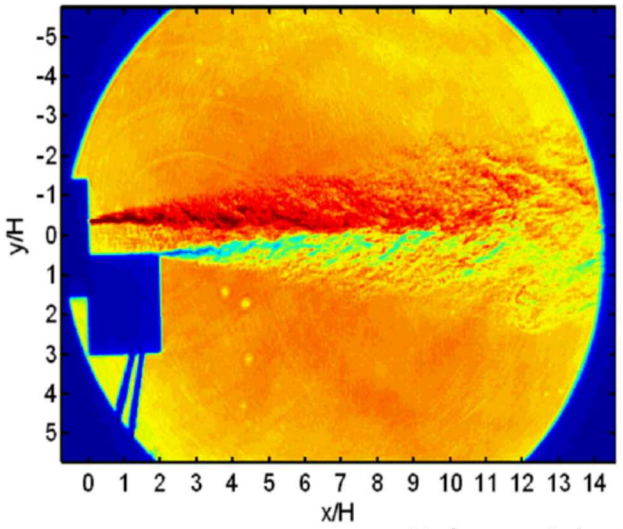

(Adamovich, 2009)

Energy deposition in flows by laser-induced plasmas

- Provides non-intrusive deposition with high energy density
- Rapid implementation allows changes in location, energy, and repetition rate
- Flow interaction time limited by the repetition rate of the laser
- Previous work has successfully implemented laser induced plasmas into supersonic flows
  - Reduce pressure forces on blunt bodies in supersonic flows; [Adelgren et al., 2005]
  - Deflect oblique shocks in supersonic inlets; [Han et al., 2002]

- Relative energy imparted into the flow; [Knight, 2008]

$$\varepsilon = {Q}\Big/{\rho_\infty C_p T_\infty V}$$

- Q: laser pulse energy (kJ)
- ρ_∞: jet exit density (kg/m^3)
- C_p: heat capacity (kJ/kg/K)
- T_∞: jet exit temperature (K)
- V: plasma volume (m^3)

- Previous work have studied laser induced plasmas with ε = 77-2100; [Adelgren et al., 2005]

Explore high-bandwidth effects of supersonic flows on pulse-burst laser-induced plasmas

Determine the conditions to sustain a pulse-burst laser-induced plasma at high Re jets

Experimental design

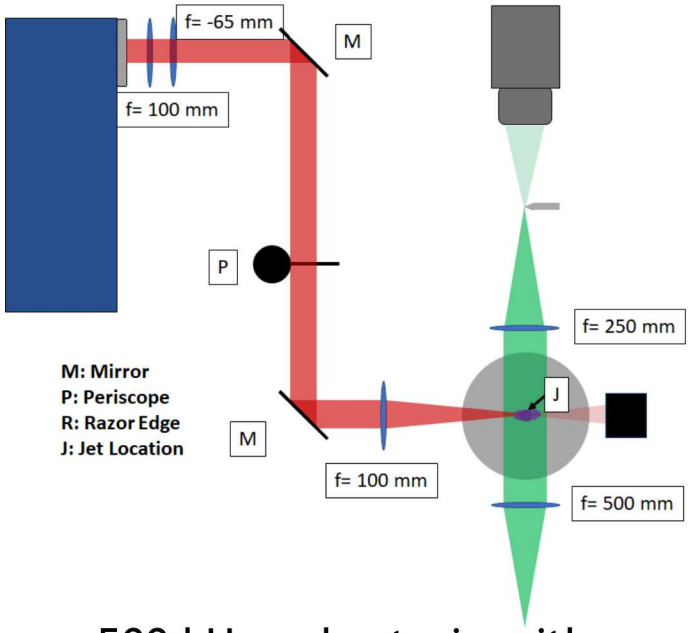

500 kHz pulse train with camera gate

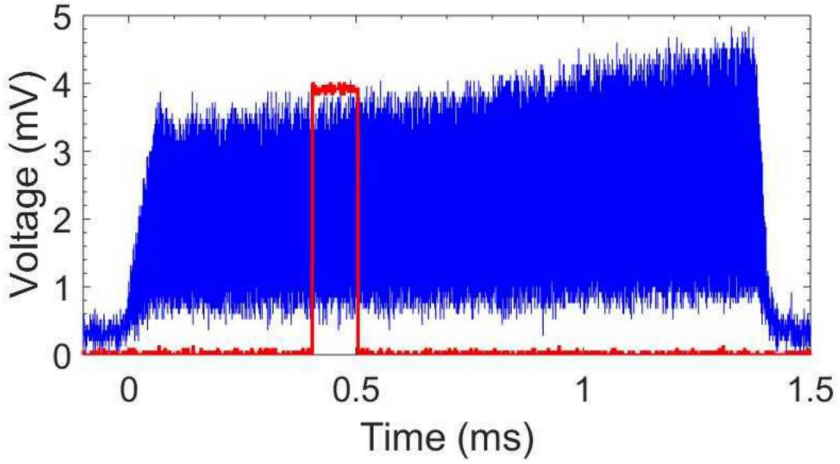

Burst rate: 5- 500 kHz, Burst duration: 1.5-10.5 ms
Total burst energy E ~ 15 J, $\varepsilon \sim 13 - 300$

Imaging of overexpanded, unperturbed jet

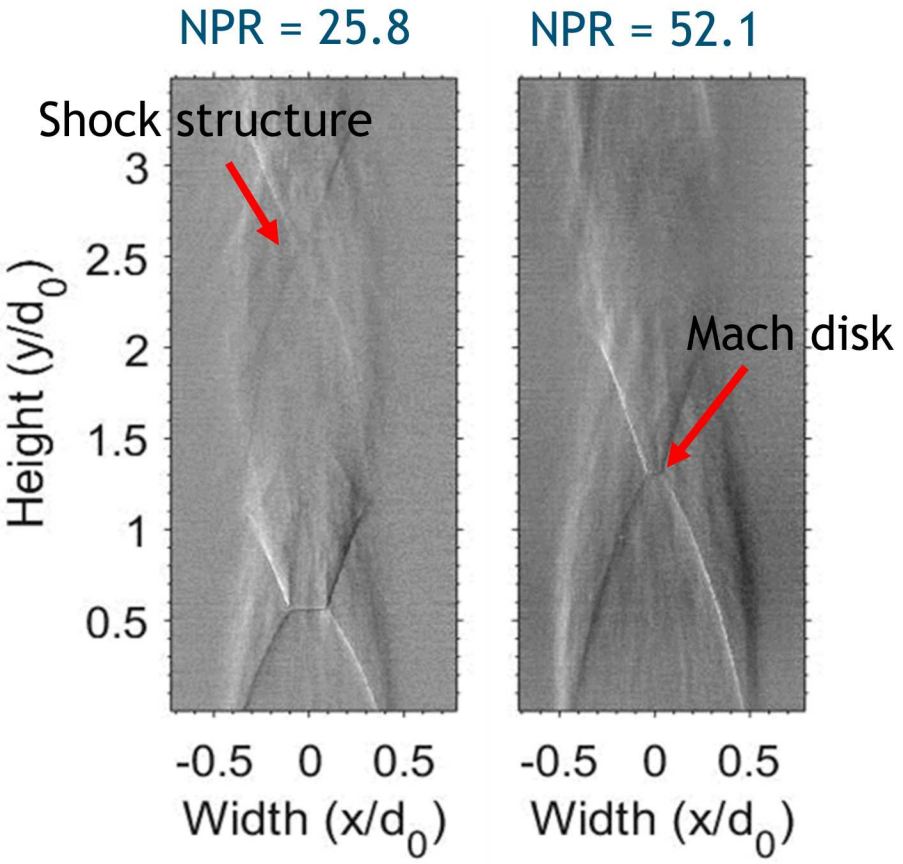

C-D nozzle, M= 3.71
Nozzle pressure ratio (NPR) ~19.5-52.1
T_{exit} = 80 K, v_{exit} = 660 m/s $d_0 = 6\ mm$

Laser-induced plasmas in quiescent air

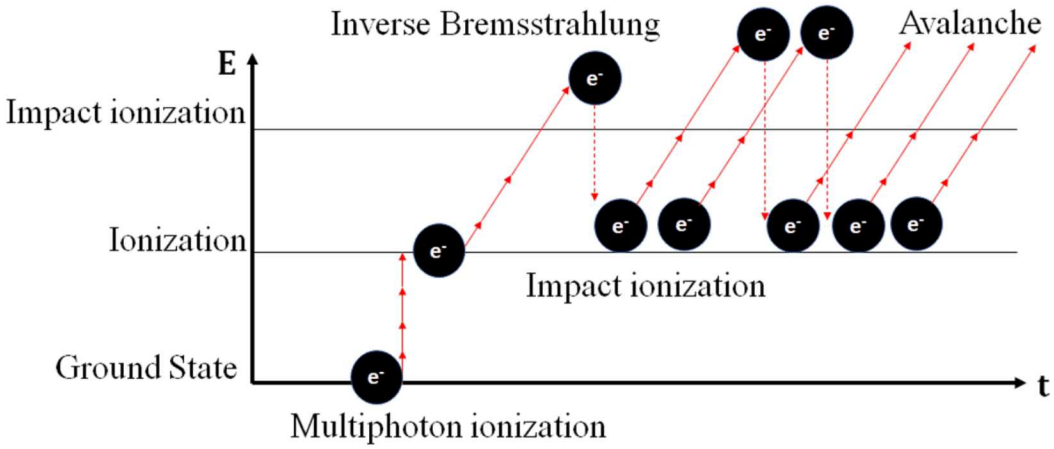

- Formation by two ionization mechanisms
  - Multiphoton → seed electron generation
  - Collisional cascade → electron avalanche
- Vortex formation generates high velocity, hot air jet
- Breakdown in air is stochastic

Plasma-induced blast wave

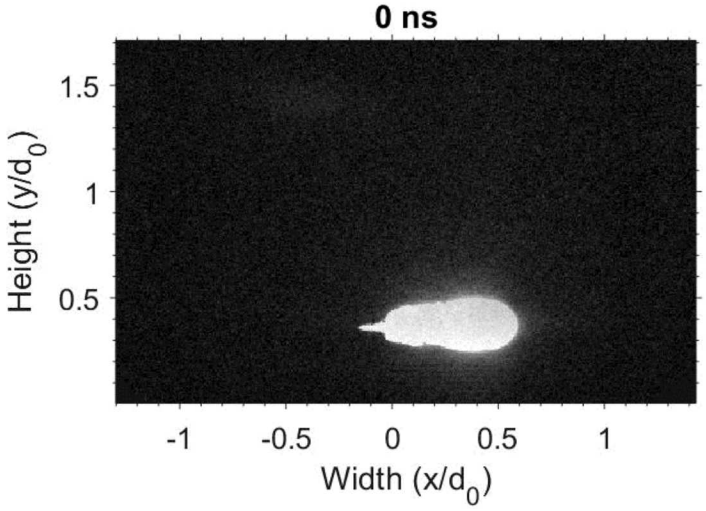

E= 310 mJ/pulse; Frame rate = 5 MHz, τ_{exp} = 10 ns

Core gas dynamics

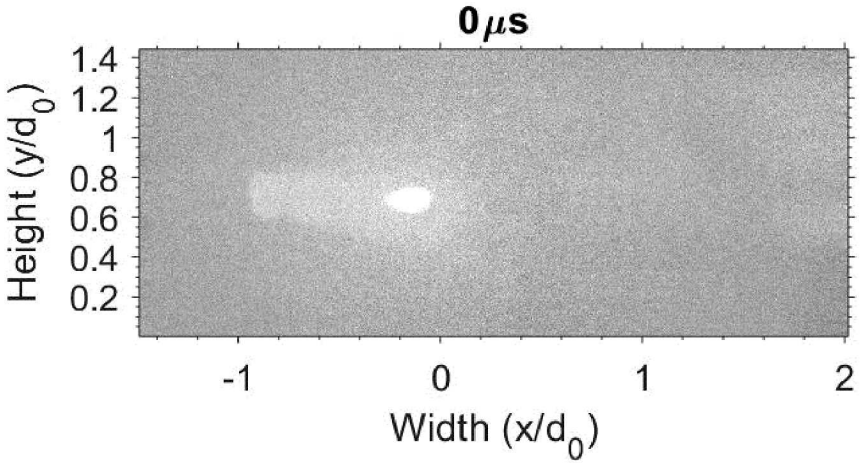

20 kHz burst rate

Frame rate = 60 kHz, τ_{exp} = 1 μs

Interaction between plasma-induced jets and supersonic flows

Location of plasma relative to jet

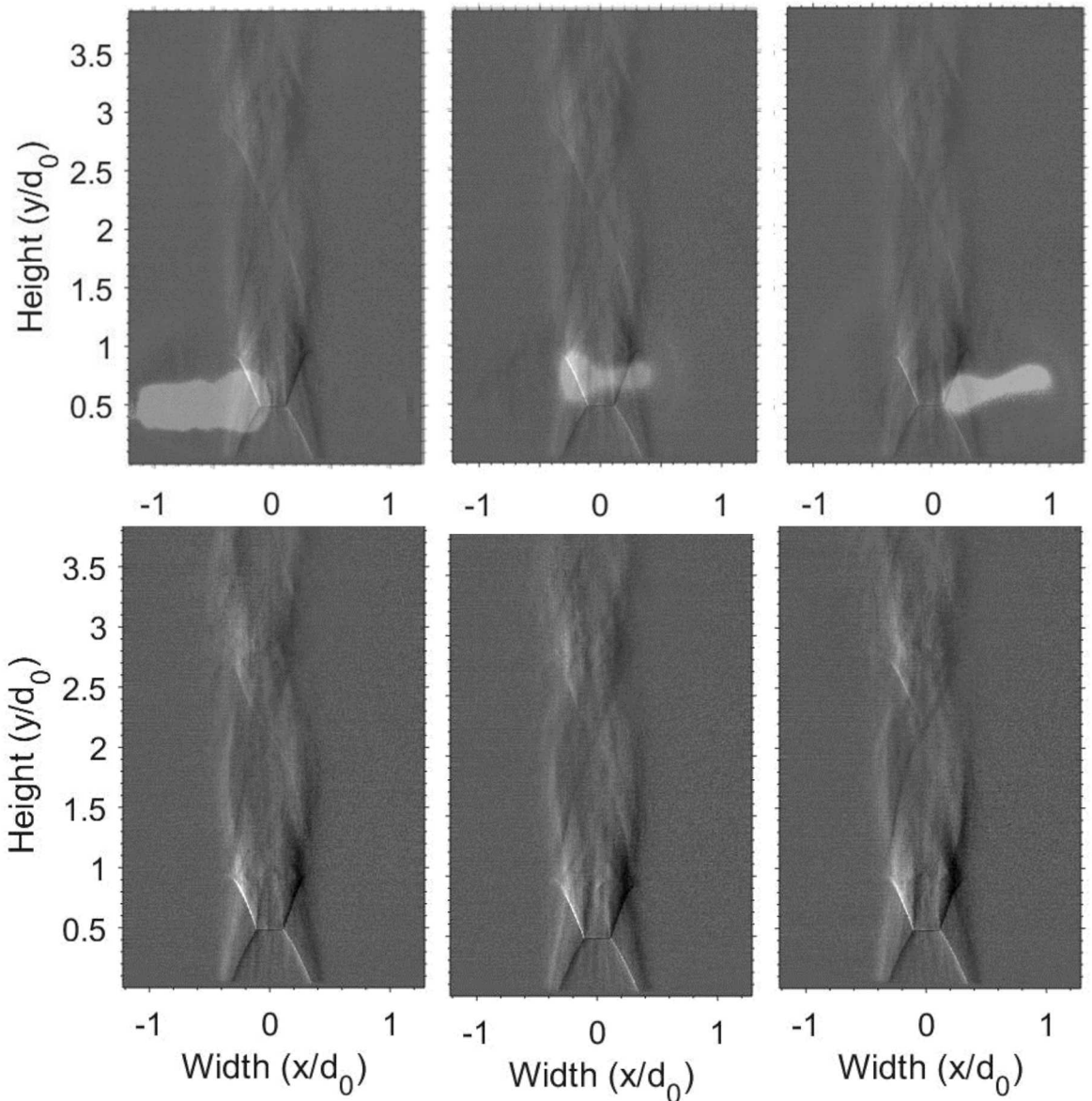

Hot air from plasma

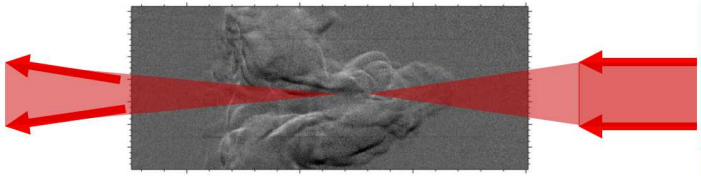

NPR= 19.2, 20 kHz burst rate

Frame rate 30 kHz

- Pushing/suction mechanism
- Collapse of the oblique shock wave
- Mach disk recovery
- Downstream shock structure
- Entrainment of hot gas

Laser pulse energy affect on jet modulation

Location of plasma relative to jet

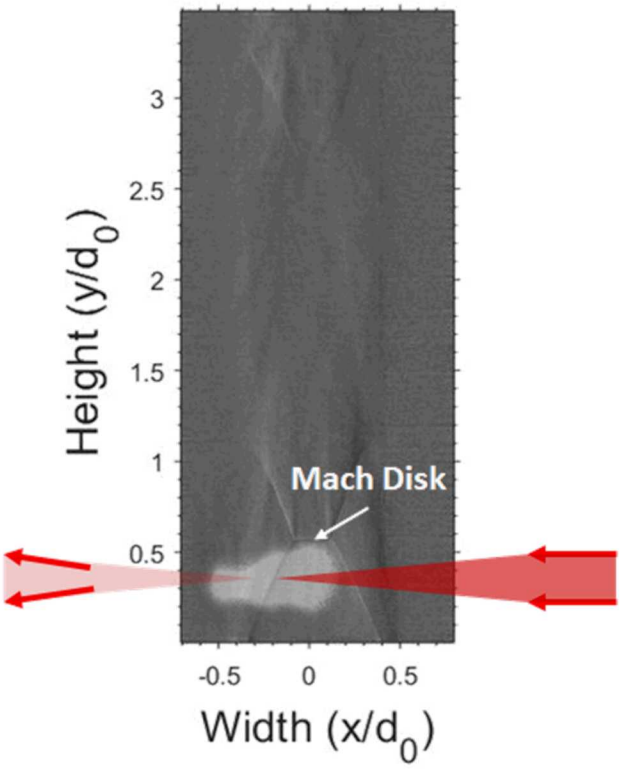

NPR= 25.9, 5 kHz burst rate

Energy variance on jet modulation

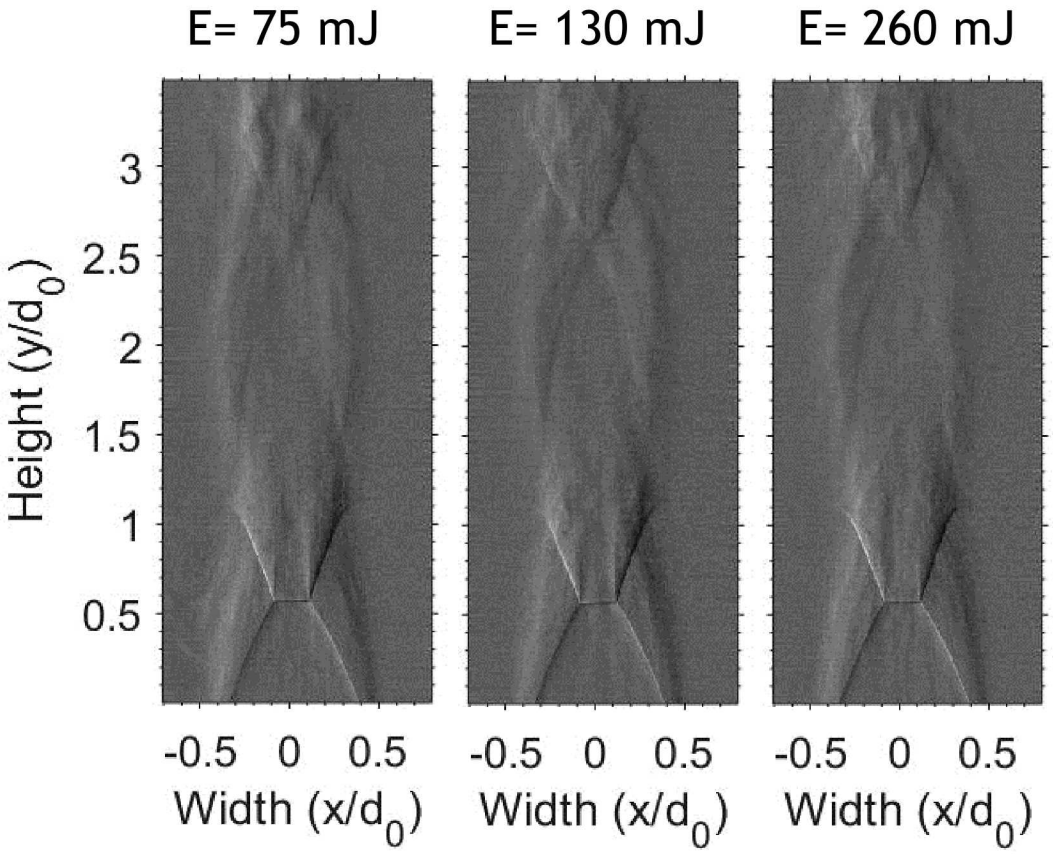

Frame rate 50 kHz, exposure 1 μs

- Low laser pulse energy effects downstream shock structure, not oblique shock waves
- High laser pulse energy is destructive to jet

Increasing laser pulse energy increase plasma volume and jet interaction

Power spectral density analysis of jet modulation by laser pulse

Regions of analysis

PSD analysis

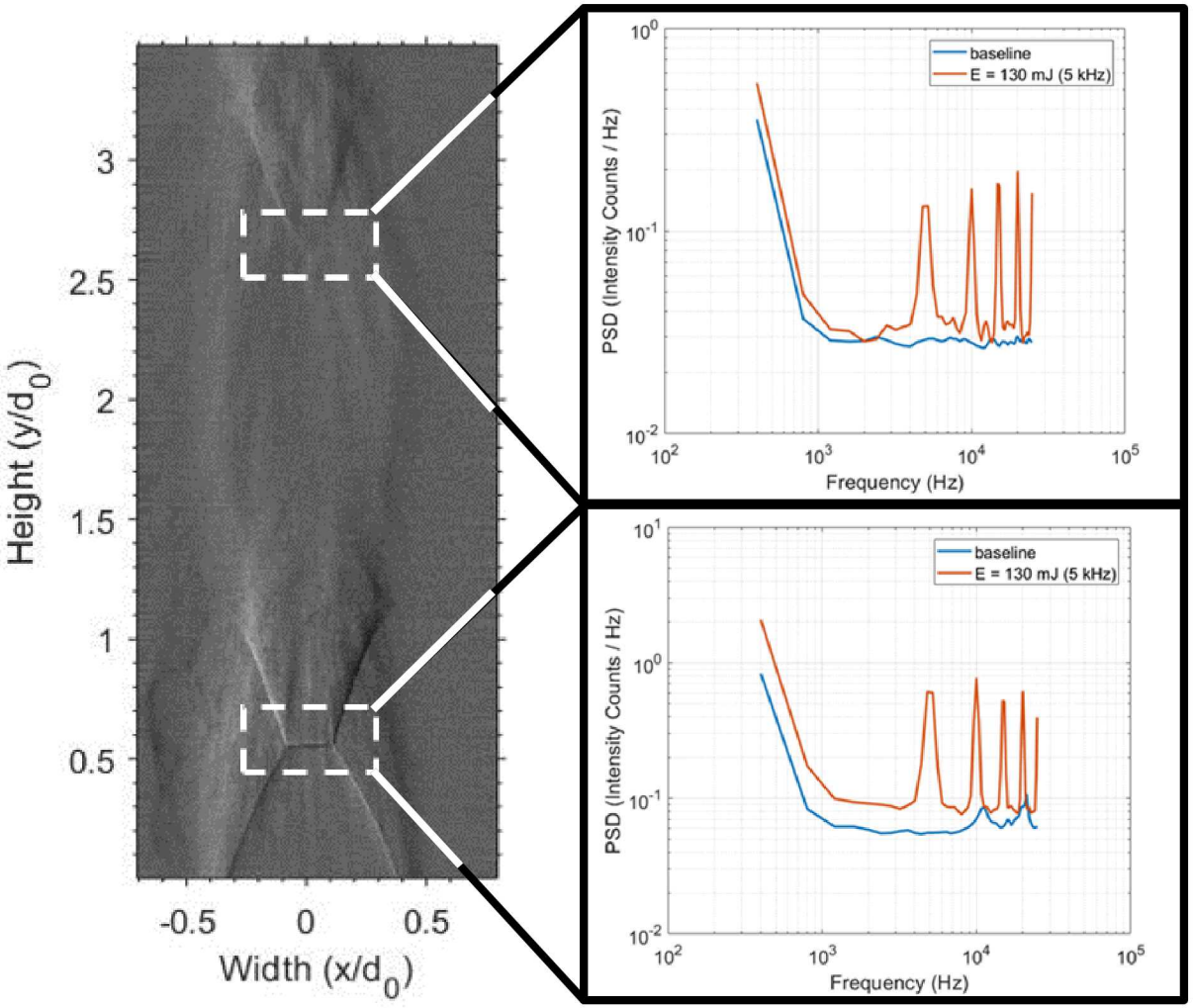

NPR= 25.9, 5 kHz burst rate
E= 130 mJ/pulse

- No analysis below 800 Hz, due to Schlieren noise limitations
- Prominent peaks
  - 5, 10, 10.5, 20, and 20.5 kHz
  - Instantaneous energy deposition
- Peaks a function of laser energy

Jet near and far fields are undulated by the laser-plasma

High repetition-rate breakdown in supersonic flow

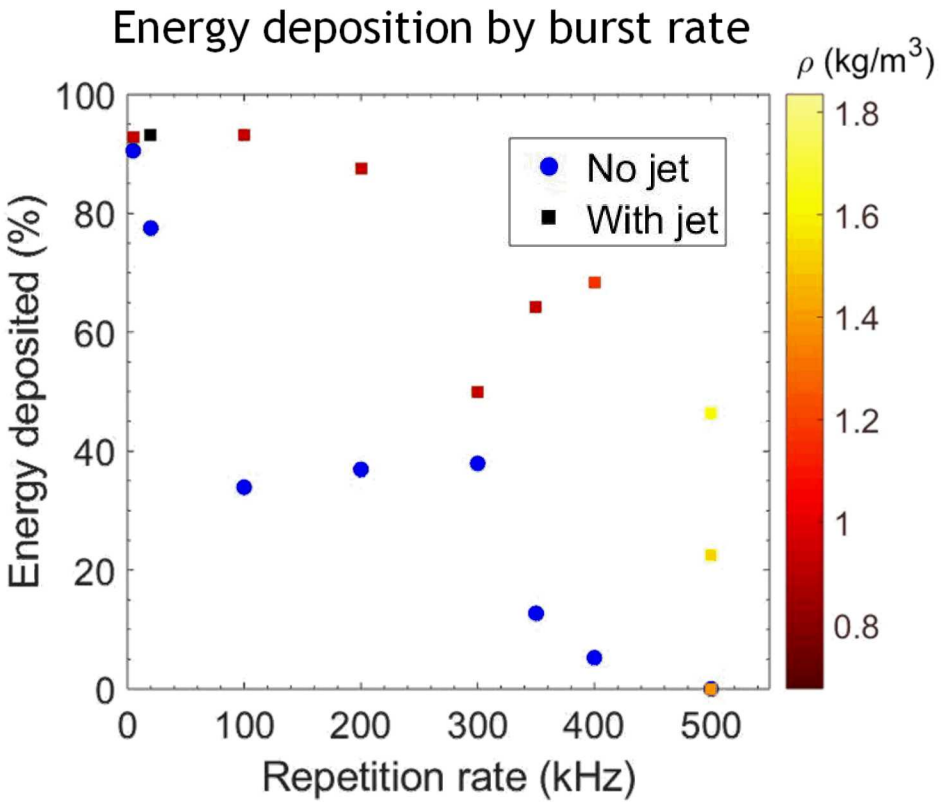

- Stochasticity in pulse-burst laser-induced plasma in quiescent air increases at higher burst rates
- Refresh rate of the supersonic jet sustains breakdown at $\tau < 350$ kHz
- Sustained breakdown at $\tau > 350$ kHz, requires both greater flow and jet exit density

Coupling pulse-burst laser-induced plasma to the supersonic jet reduces stochasticity

High-bandwidth laser-plasma/jet-flow interactions

Unperturbed jet, NPR = 52.1

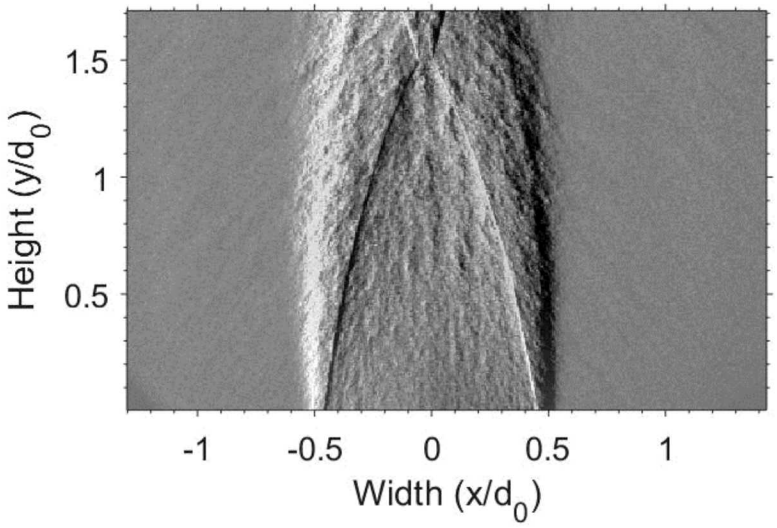

500 kHz burst rate

Frame rate 5 MHz, exposure 10 ns

- High repetition breakdown in the flow
- Permanent jet modulation
- Continuous plasma emission at the jet core
- Shock re-excitation of plasma species

Permanently disrupted jet

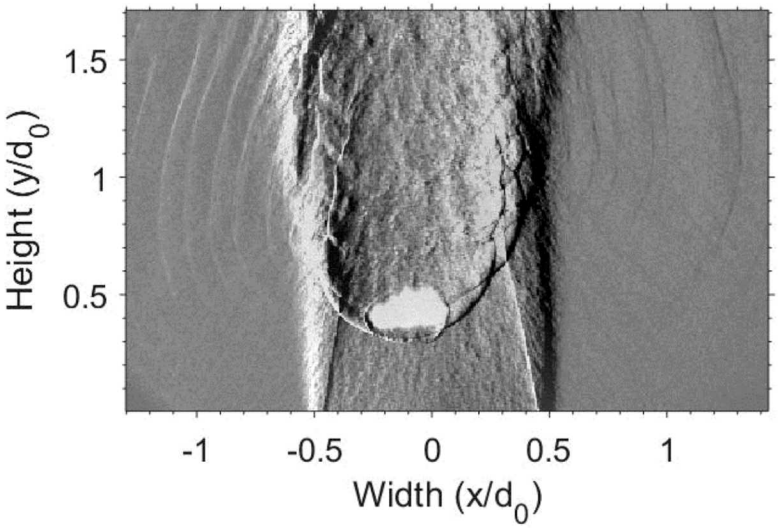

N(II) emission in jet core

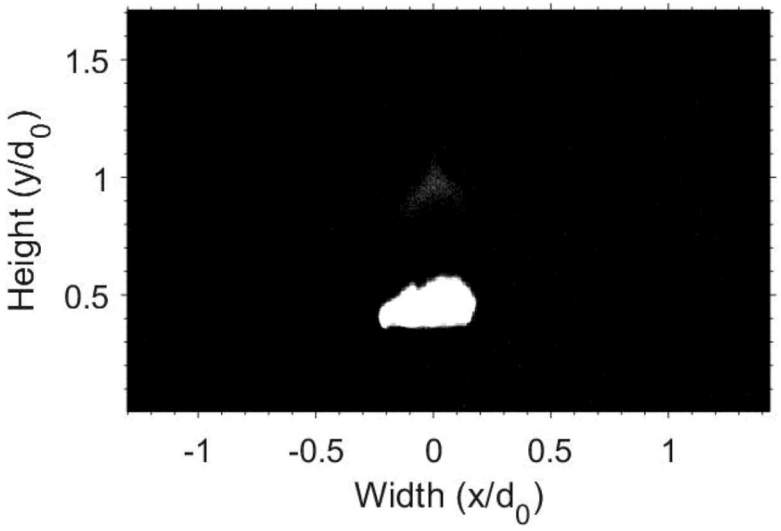

Implications for supersonic plasma ignition

N(II) emission in jet core

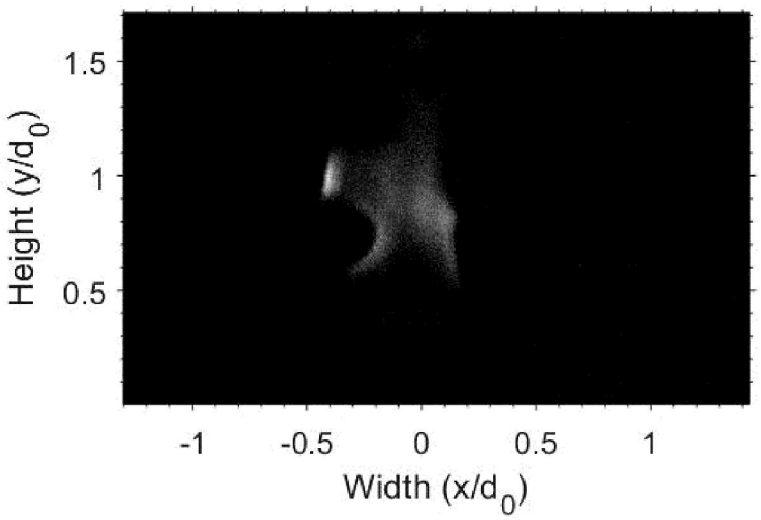

300 kHz burst rate

Frame rate 5 MHz, exposure 100 ns

Repeatability of plasma convection

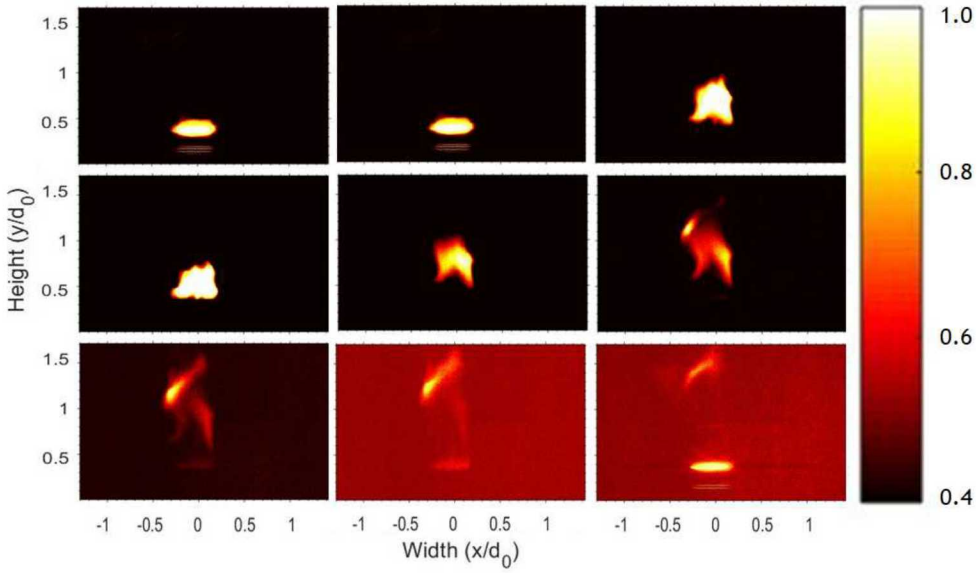

- Plasma is stretched during convection
- Path of convection is repeatable
- Plasma kernel interaction length
  - 300 kHz: 4.8 mm
  - 500 kHz: 3.0 mm

Ultrafast laser-induced breakdown spectroscopy (LIBS)

Variance throughout the burst

$\sigma^2 = 3.8507$

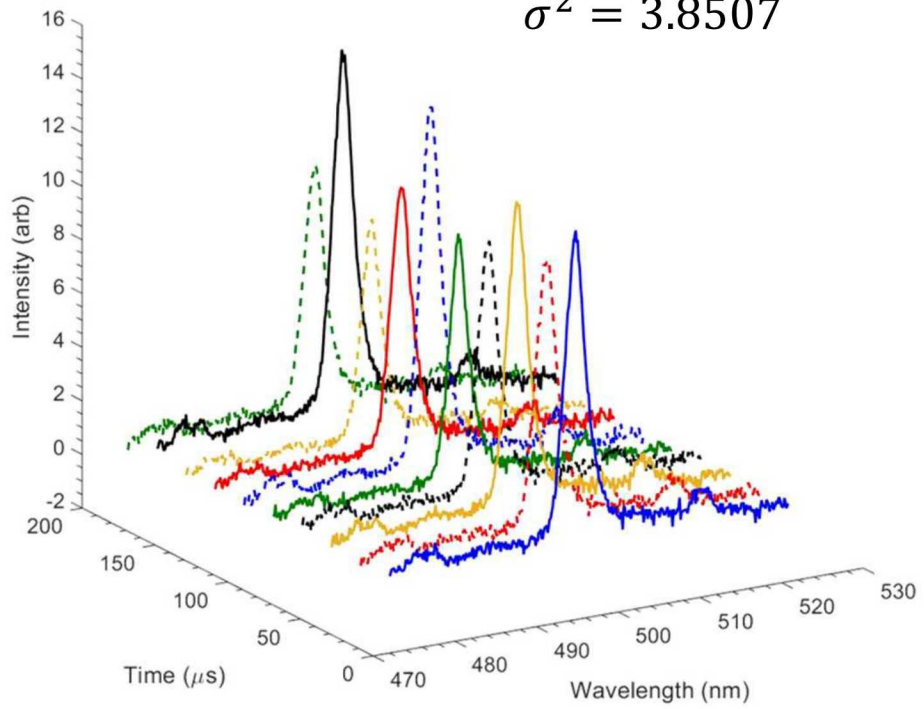

Time evolution of single LIP

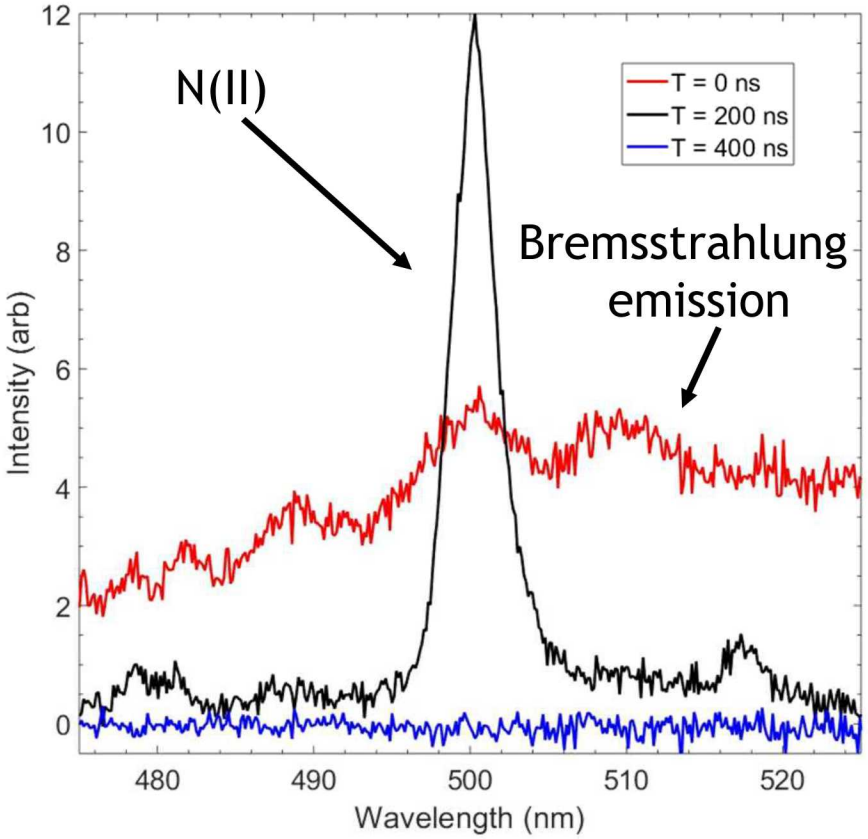

- Plasma varies shot-to-shot throughout burst
- Plasma initially has broadband emission from electron recombination processes
- Strong spectral features appear as plasma is decaying
- By 400 ns after breakdown, plasma no longer emits

Preliminary temperature measurements

N(II) Emission

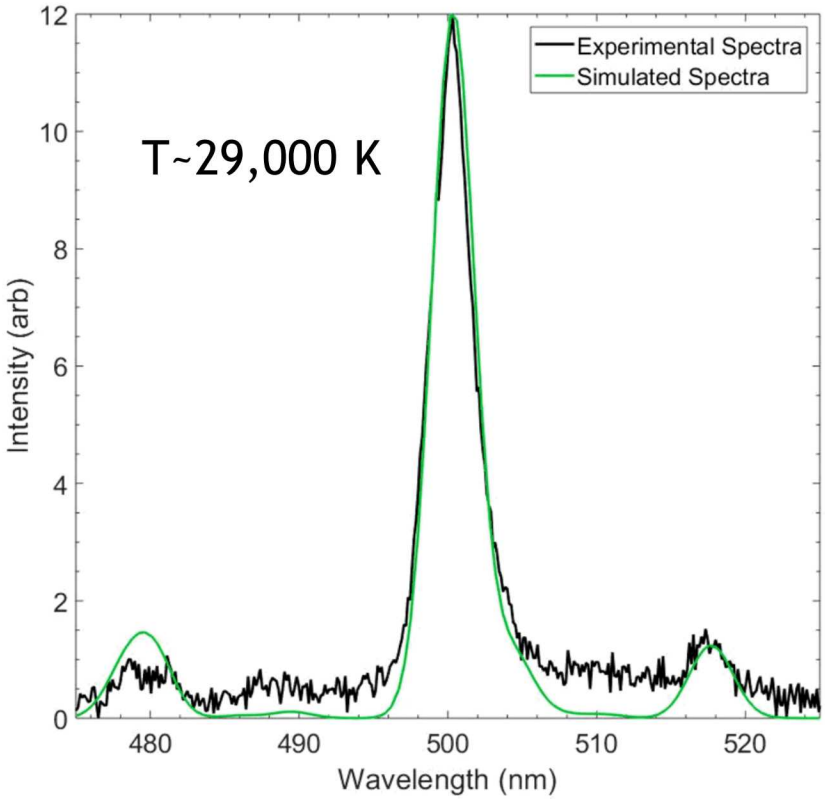

E= 17 mJ/pulse; Burst rate= 500 kHz;
Frame rate = 5 MHz, τ_{exp} = 100 ns

- Spectra was fit using NIST LIBS database
- Chip dispersion ≈ 0.1357 nm/pixel
  - Signal-to-noise tradeoff with resolution
- N_e~ 1e18 cm^{-3}, assumed from previous work
- Peak emission (λ~500 nm) → ^3S, ^5P, ^3D states
  - E_u ~187,000 to 226,000 cm^{-1}
- Secondary emission (λ~518 nm) → $^5P°$, $^5D°$ states
  - E_u~244,000 cm^{-1}
- Sources of uncertainty
  - Only ionized nitrogen present in spectra
  - Raised baseline in fit

Conclusions Part II

- At all repetition rates, the presence of the jet was found to be critical and beneficial to repeatable plasma breakdown.
- Substantial deflection of supersonic, oblique shock waves was achieved with a laser focus prior to the jet, within the jet and on the far side of the jet.
- Increasing pulse energy increased the hot gas core/flow interaction time, but the increase in plasma volume caused a more destructive blast-wave/jet interaction.
- Spectral analysis at E = 130 mJ/ pulse showed strong modulation of the jet in the near field Mach disk and the far field shock train
- N(II) emission imaging at 5 MHz demonstrated a 500 kHz burst could generate a near continuous plasma held in the core flow.
- High burst rate laser-induced plasmas cause permanent, controllable actuation of the flow for the entire burst period, and this actuation has significant implications for non-intrusive, plasma flame holding

High Energy Arc Faults

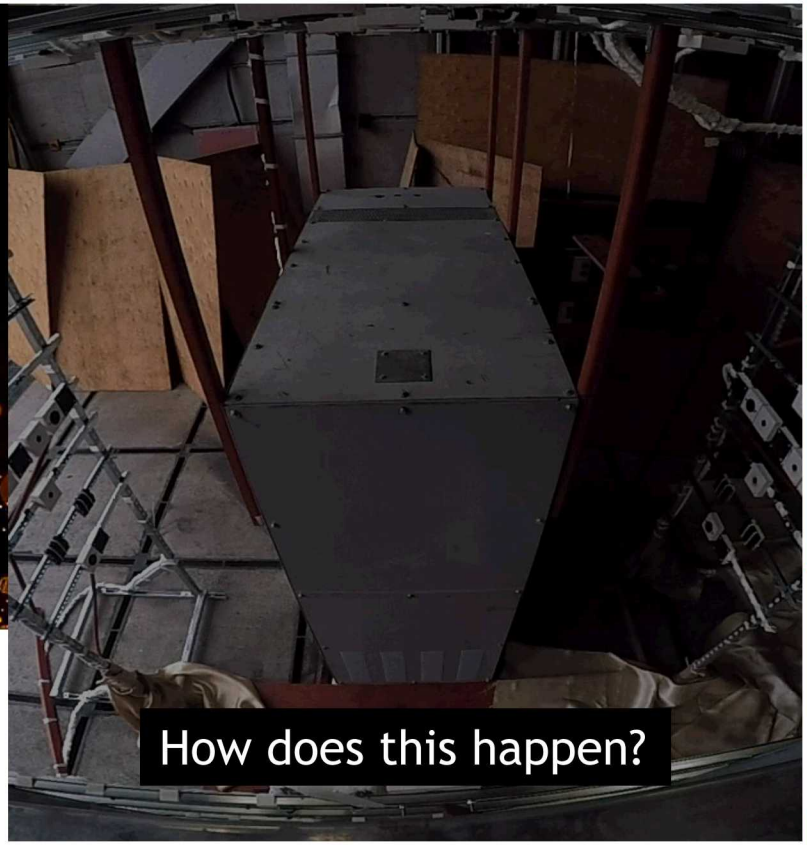

- The dominant modes of energy transfer from DC arc → cabinet and arc → jet are unknown
- Well defined jetting mechanisms are critical to informing hazard mitigation
- Plasma's "zone of influence" encompasses heat and spectral exposure

Small-scale physics for large-scale problem

Arc energy transfer mechanisms

$$q''_{rad} = \sigma\varepsilon(T^4 - T_\infty^4)$$

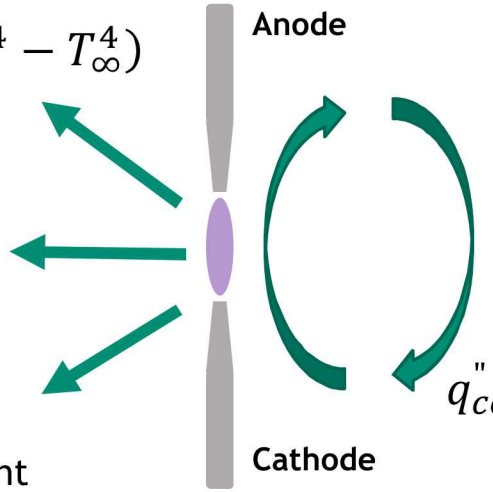

$$q''_{conv} = h_f(T - T_\infty)$$

h_f: film coefficient

σ: Stefan-Boltzmann constant

ε: emissivity

Aluminum arc jet

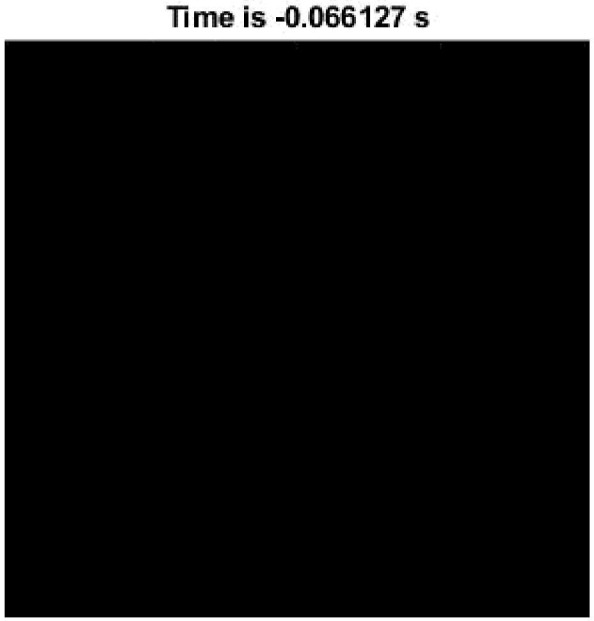

Challenges

- Evaluating emissivity and film coefficient
- Determining emissive and convective surface areas
- Understanding DC arc parameters: electron number density, temperature
- Measuring bulk jet parameters: conductivity, velocity, temperature, etc.

Need stable, well characterized arcs to understand physics of source plasma and arc jets

HEAF testbed and diagnostics set-up

Experimental Schematic

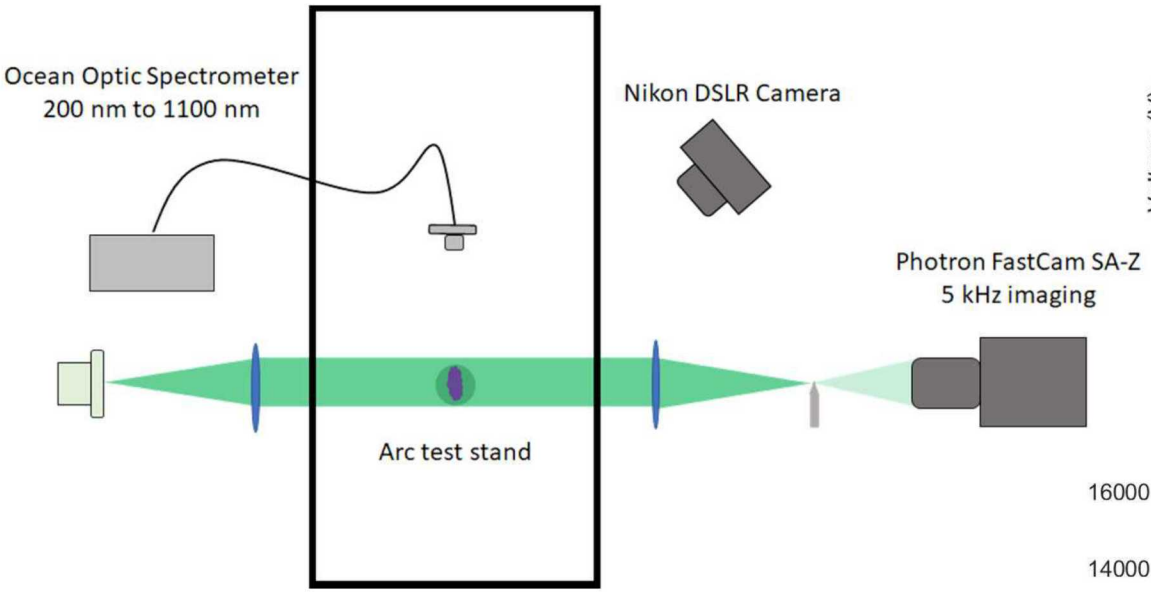

Traces from DC power supply

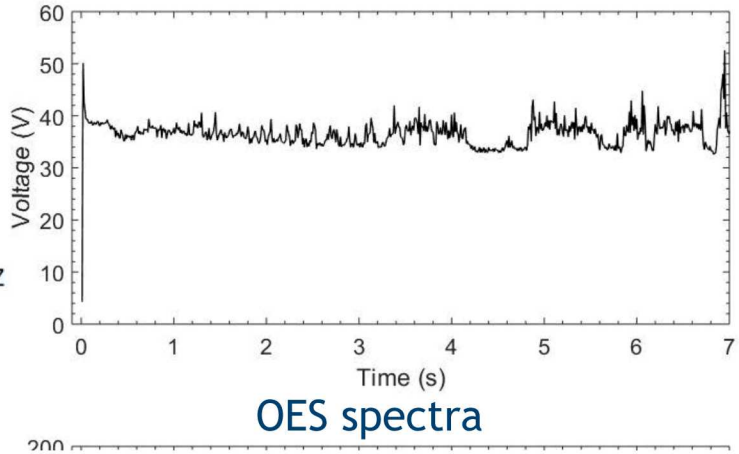

OES spectra

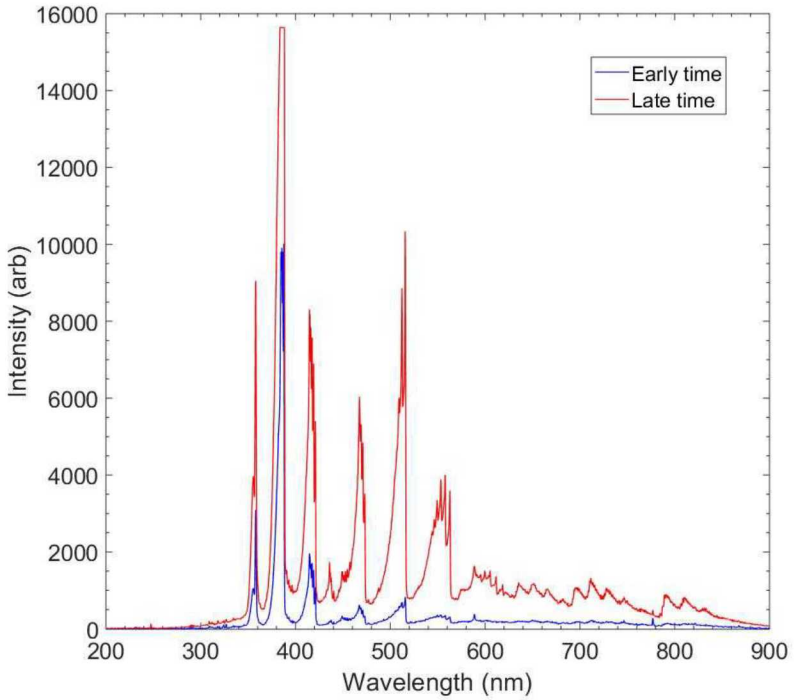

Optical emission spectroscopy

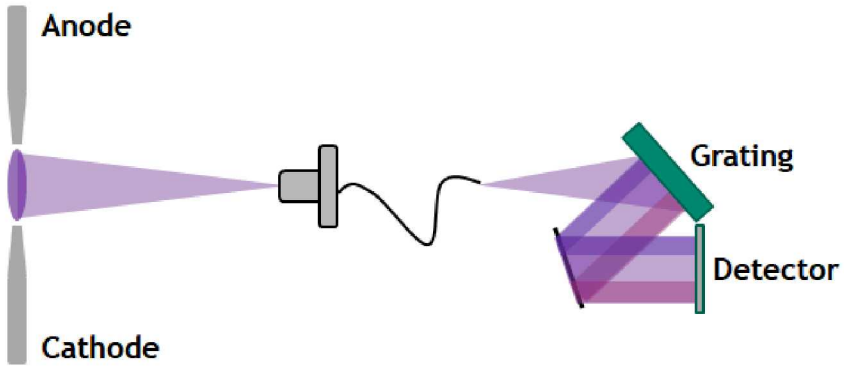

Analyzing spectra: what can emission tell us?

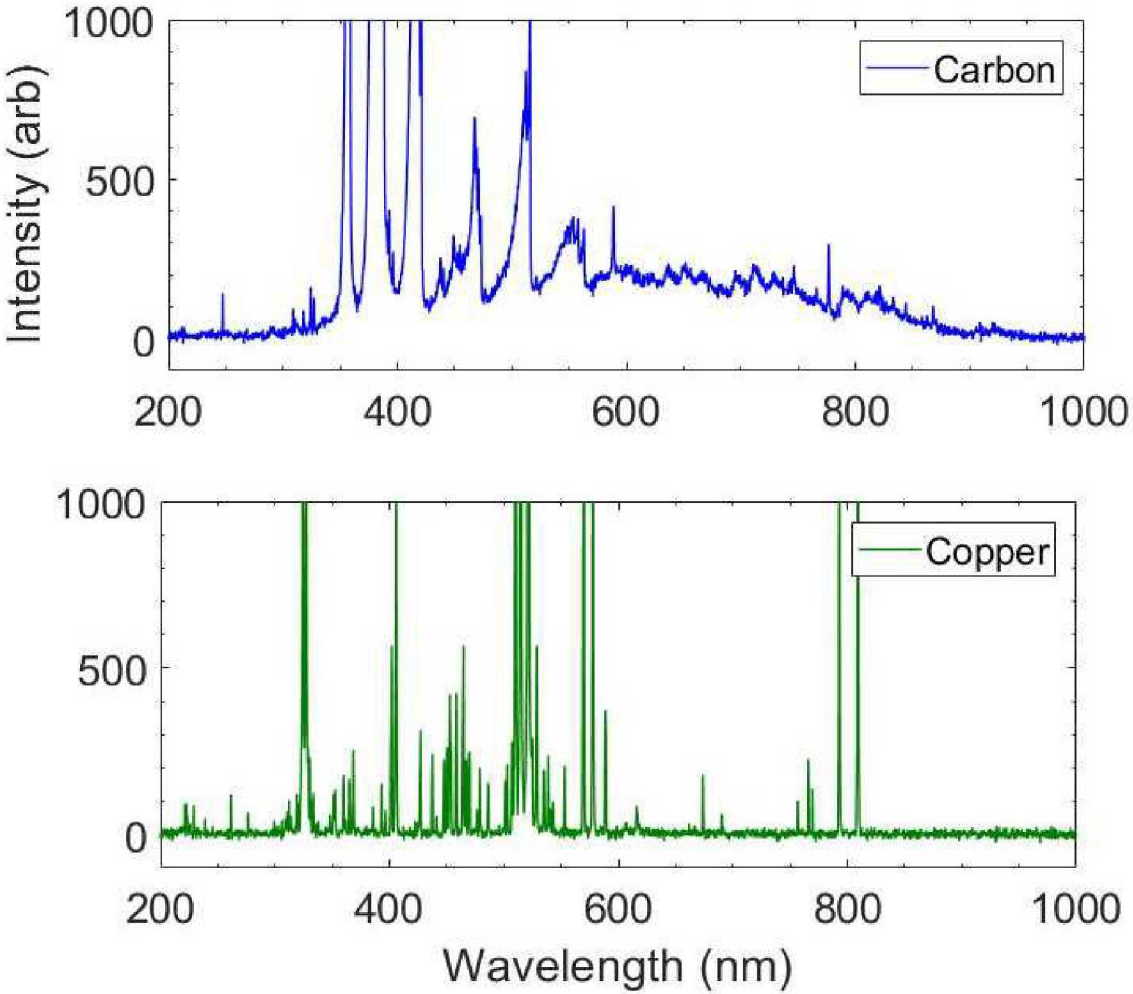

100 Hz acquisition rate, Ocean Optics

- Is there a raised baseline?
  - Emitter has a graybody component to it (although graybody assumption might not be best)

Analyzing spectra: what can emission tell us?

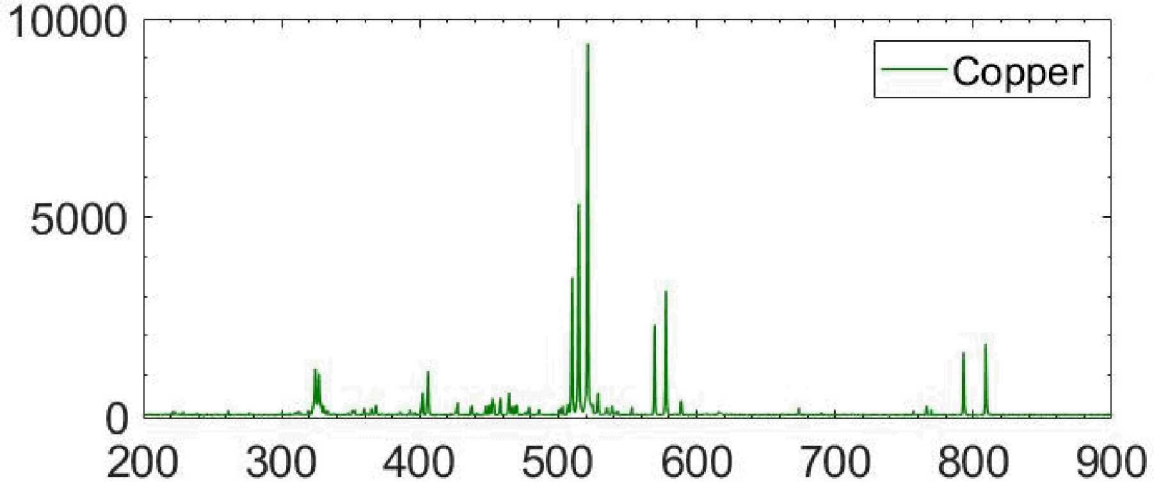

- Atomic and/or molecular features?
  - Atomic emission is two-step process
    - Dissociation
    - Excitation

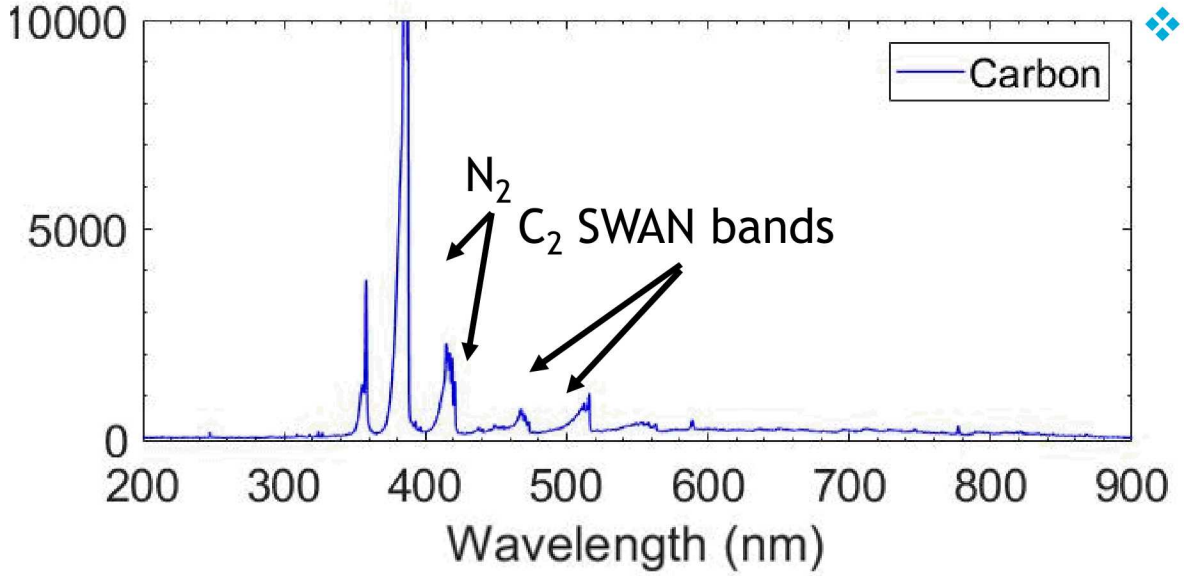

- Atomic and/or molecular features?
  - Molecules emit from both vibrational and rotational energy states
    - As temperature increases, more vibrational bands are excited
    - Temperature also changes the manifold structure (shape of the vibrational band)

Spectral temperature analysis: broadband emission

Tungsten lamp calibration

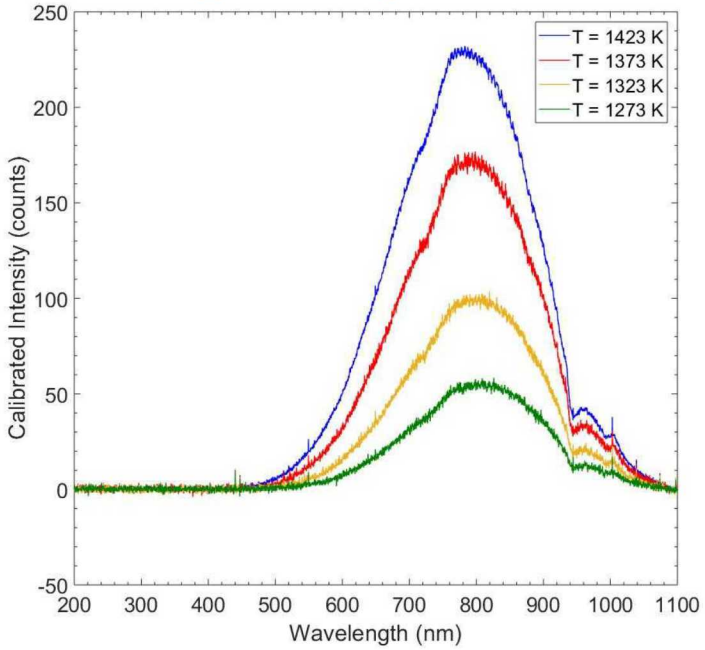

Spectral baseline fit

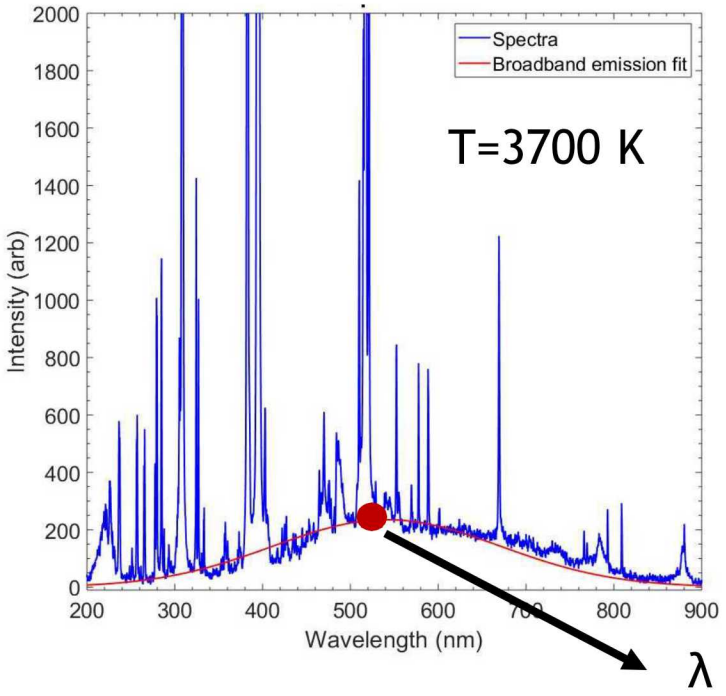

$\lambda = -a*T + b$

- Blackbody source, tungsten lamp, calibrated the baseline "plateau" emission
- Calibration completed from 1000-3000 K

From Wein's Law, the wavelength of highest intensity is directly related to the temperature

Spectral temperature analysis: Boltzmann plot of metallic atoms

$$I = \frac{h\nu AN}{4\pi} = \left(\frac{hcN_0gA}{4\pi\lambda Z}\right)e^{-E_u/kT} \longrightarrow \ln\left(\frac{I\lambda}{gA}\right) = \frac{-E_u}{kT} - \ln\left(\frac{4\pi Z}{hcN_0}\right)$$

E_u: upper level energy
k: Boltzmann constant
A: transition probability
g: upper level degeneracy
λ: wavelength
I: measured transition intensity

- Assume local thermal equilibrium (LTE)→ fast, ~100 ns at P = 1 atm
- Ex: Cu-air plasma

Wavelength (nm)	Upper energy (cm^{-1})
570	30783
578	30535
793	43137
809	43137

Boltzmann plot

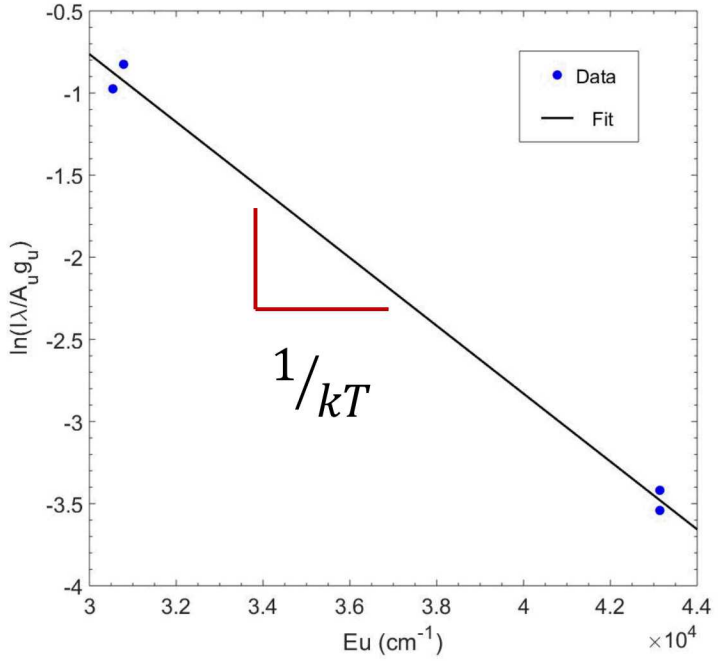

- Measurement sensitivity ↑ with more energy levels
- Interference is reduced by choosing isolated features

Comparison of inferred temperature measurements

Copper arc, I = 100 A

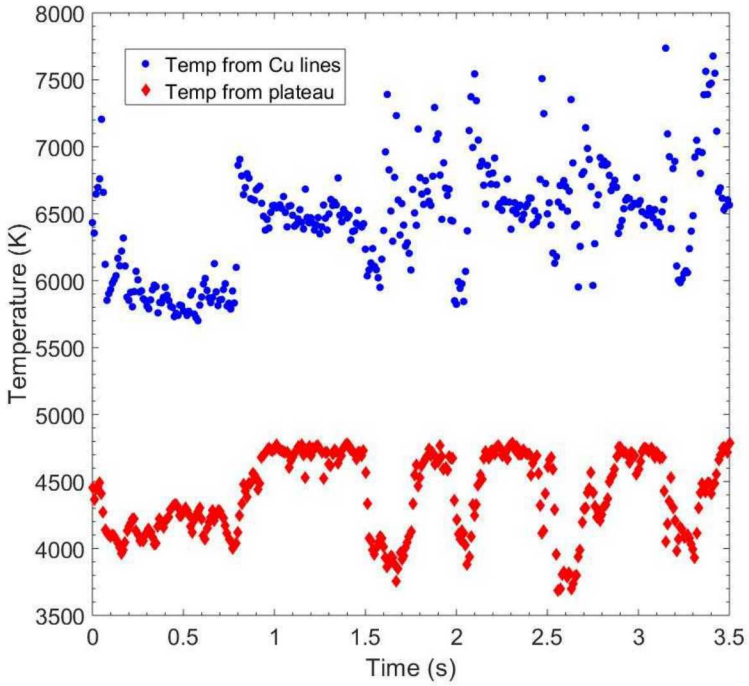

Maximum Std. Error of Estimate

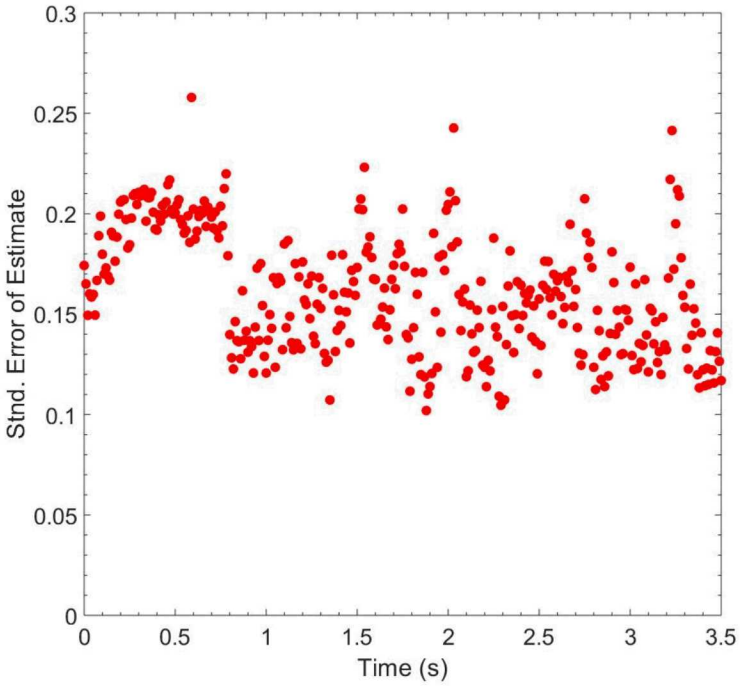

- Temperature inferred from broadband emission is lower than temperature of metallic atoms
- Instabilities in the arc effect the BBR temperature more significantly that the Cu vapor temperature

Effect of arc stability on Al emission spectra

Al arc emission image

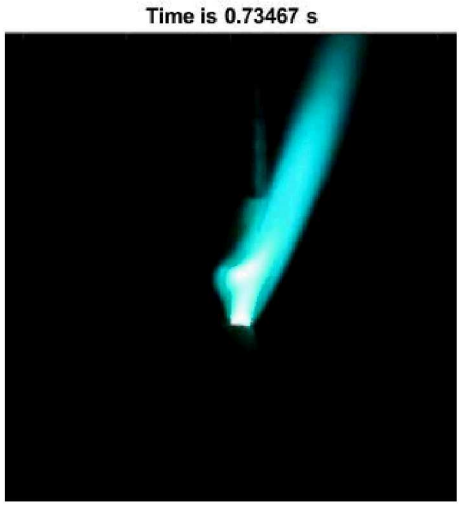

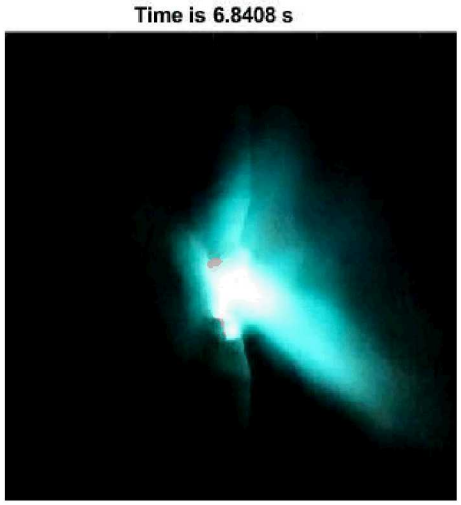

Al arc emission spectra

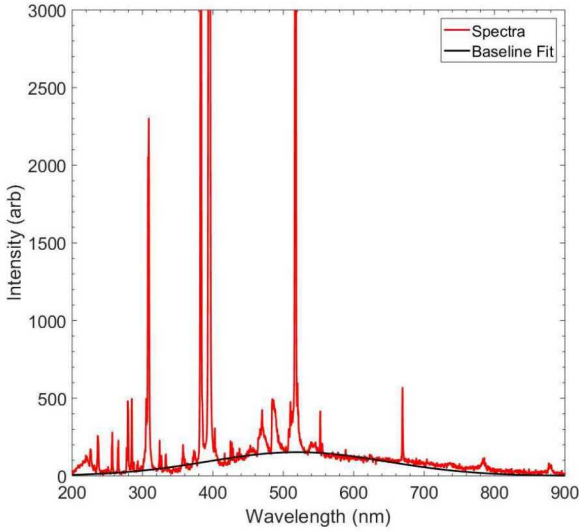

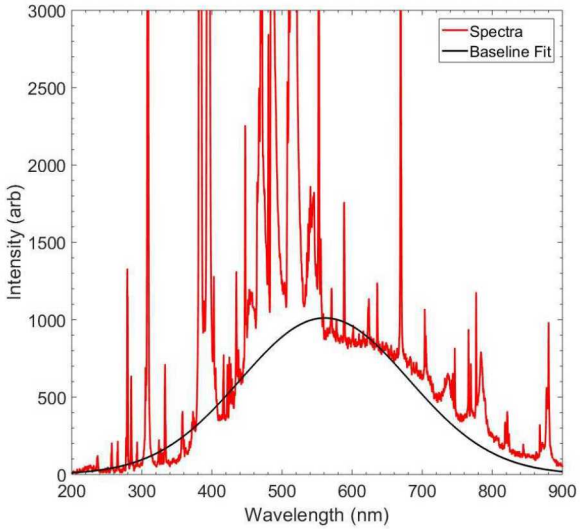

- "Stable" features appear to have the same plateau emission
- "Unstable" features show contributions from hot gas core and colder, re-radiating surrounding gas

Does graybody assumption hold for DC source?

Effect of arc stability on inferred temperature

Dependence of arc location on temperature

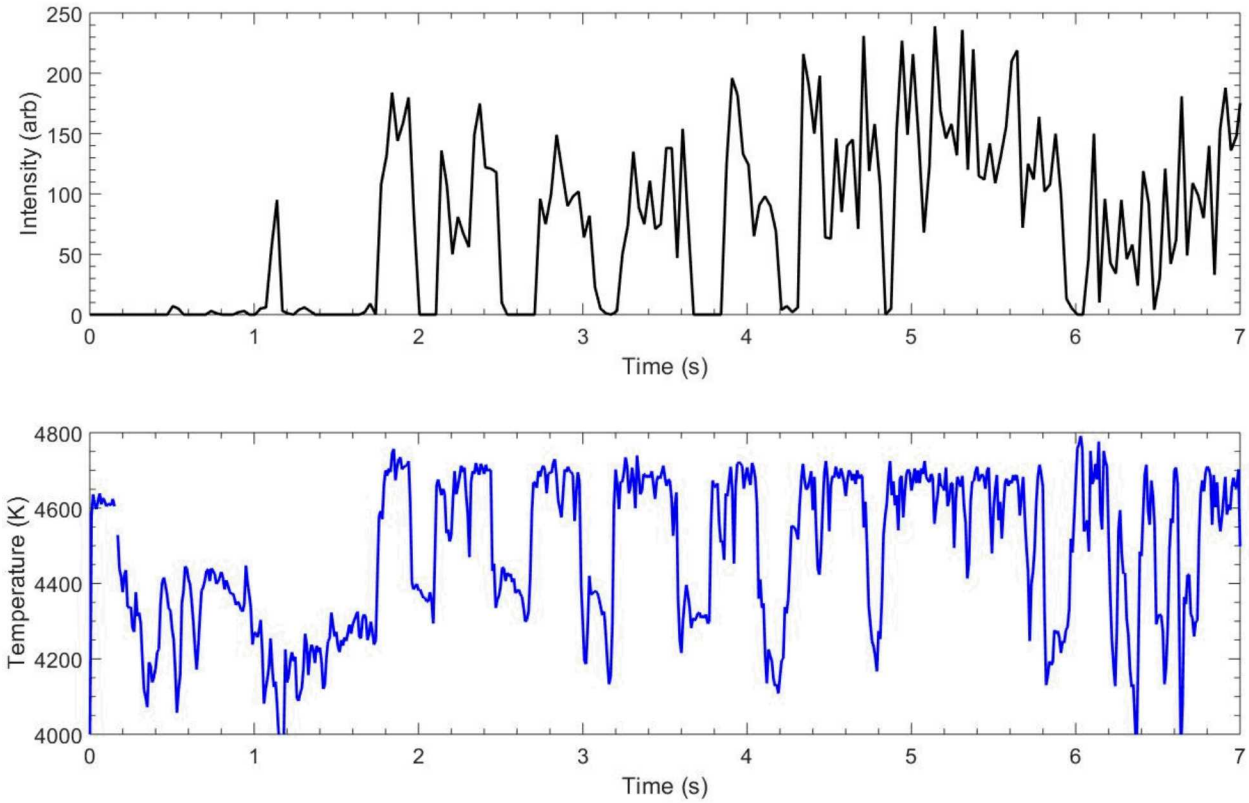

Al arc emission

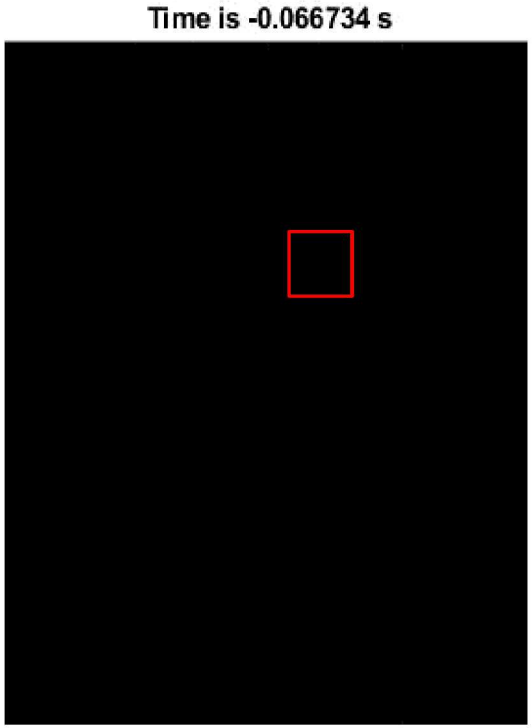

- When the arc jet encompasses the anode, a hotter blackbody radiator is inferred

Convective flow field comparisons via Schlieren imaging

Development of copper flow field

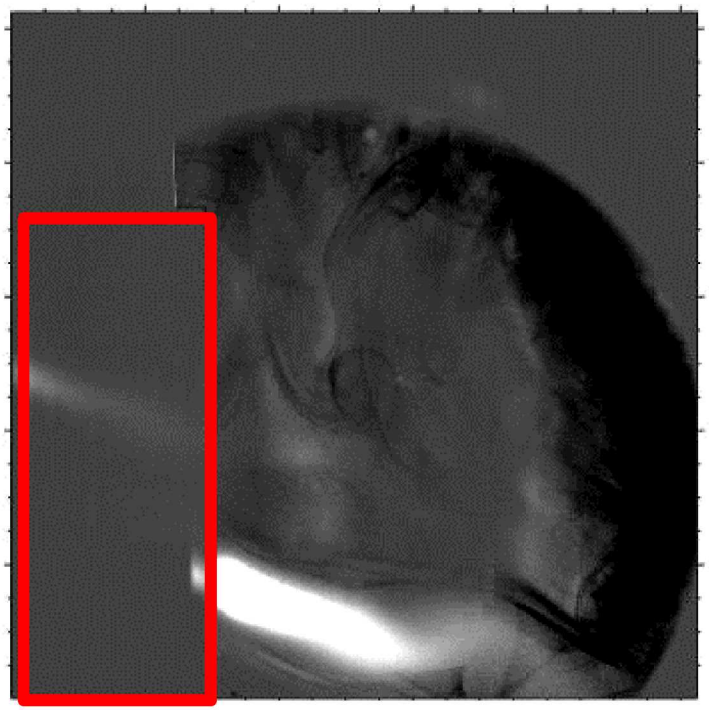

Development of aluminum flow field

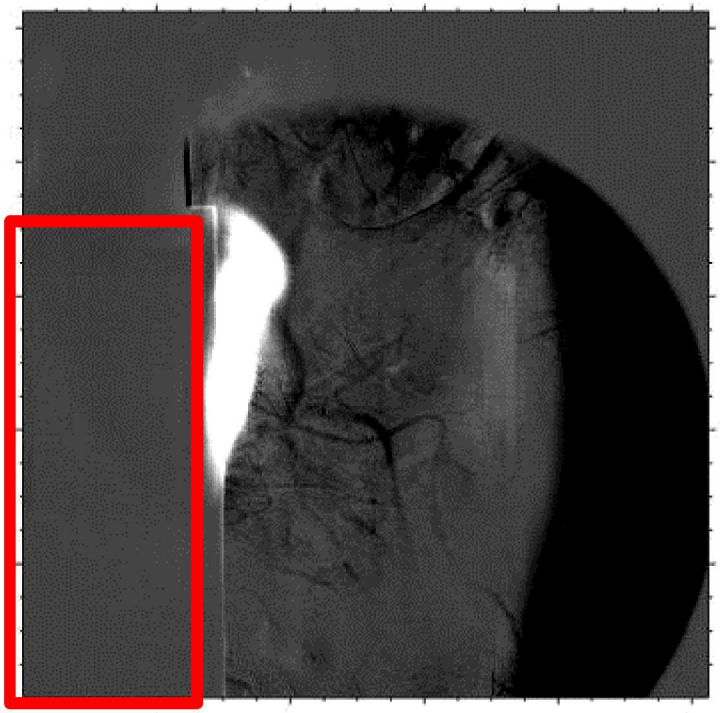

- Mask (red box) limits arc emission, for better contrast and protects the camera from burning
- Copper jet demonstrates convective heat transfer to surrounding gas
- Aluminum jet shows burning particulates, soot formation, and convectively heated gas

Conclusions Part

- A DC arc produces a jet, which has varying stability with electrode geometry
- The variance of the arc jet location effects the inferred graybody temperature more than temperatures inferred from spectral emissivities
- Temperature inferred from a Boltzmann plot is significantly higher than temperatures inferred from broadband emission
- Differing inferred temperatures implies that spectra is convoluted; holding both DC plasma emission and re-radiating gas emission
- Knowledge of power radiated versus power convected by the arc is critical to understanding how high energy arc faults will effect their surrounding.

Acknowledgements

We gratefully acknowledge Sandia National Laboratories and the Laboratory Directed Research and Development (LDRD) program, EPRI and the NRC for funding this research

Great thanks for the support and advice from:

- Justin Wagner
- Steven Beresh
- Marley Kunzler
- Seth Spitzer
- Ed DeMauro
- Danny Kotovsky
- Paul Clem
- Ray Martinez
- Chris Murzyn
- Michael Clemenson

Continuing work

- Stark broadening for electron number densities in the plasmas
- Metallic vapor concentration calculations
- Comparison of graybody emissivities
- Comparison of spectral emissivities
- Power radiation calculations